AEM Journals.ASM.org

Evolutionary Engineering Improves Tolerance for Replacement Jet Fuels in *Saccharomyces cerevisiae*

Timothy C. R. Brennan,[a] Thomas C. Williams,[a] Benjamin L. Schulz,[c] Robin W. Palfreyman,[a] Jens O. Krömer,[b] Lars K. Nielsen[a]

Australian Institute for Bioengineering and Nanotechnology, University of Queensland, Brisbane, Queensland, Australia[a]; Centre for Microbial Electrochemical Systems (CEMES), Advanced Water Management Centre (AWMC), University of Queensland, Brisbane, Queensland, Australia[b]; School of Chemistry and Molecular Biosciences, University of Queensland, Brisbane, Queensland, Australia[c]

Monoterpenes are liquid hydrocarbons with applications ranging from flavor and fragrance to replacement jet fuel. Their toxicity, however, presents a major challenge for microbial synthesis. Here we evolved limonene-tolerant *Saccharomyces cerevisiae* strains and sequenced six strains across the 200-generation evolutionary time course. Mutations were found in the tricalbin proteins Tcb2p and Tcb3p. Genomic reconstruction in the parent strain showed that truncation of a single protein (tTcb3p$^{1-989}$), but not its complete deletion, was sufficient to recover the evolved phenotype improving limonene fitness 9-fold. tTcb3p$^{1-989}$ increased tolerance toward two other monoterpenes (β-pinene and myrcene) 11- and 8-fold, respectively, and tolerance toward the biojet fuel blend AMJ-700t (10% cymene, 50% limonene, 40% farnesene) 4-fold. tTcb3p$^{1-989}$ is the first example of successful engineering of phase tolerance and creates opportunities for production of the highly toxic C_{10} alkenes in yeast.

Monoterpenes are 10-carbon (C_{10}) terpenes derived from two C_5 isoprene units (1). Traditionally used in the flavor and fragrance industry, monoterpenes, such as *d*-limonene, are now also sought after as precursors for light end components of "drop-in" jet fuels (2). With the ability to convert simple sugars into a variety of enantiomerically pure monoterpene products (3–5), microbial synthesis has the potential to overcome the low yields, impurities, and high costs associated with conventional chemical synthesis or extraction from biological tissues (6). The C_{15} sesquiterpene farnesene is currently produced via fermentation of *Saccharomyces cerevisiae* for diesel markets (N. Renninger and D. McPhee, U.S. patent application WO2008045555 A2). Monoterpenes and sesquiterpenes are both derived from the mevalonate pathway, indicating that yeast has the potential to provide sufficient carbon, redox power, and energy to produce commercial quantities of monoterpenes. Unlike sesquiterpenes, however, monoterpenes are highly toxic. In *S. cerevisiae*, for example, limonene halts growth at 60 mg/liter (2). Since maximizing titers is an absolute requirement for cost-effective production (7), toxicity is a critical challenge facing microbial monoterpene production and biotransformation (8).

Because monoterpenes are oils, they are sparingly soluble in water and cause phase toxicity rather than molecular toxicity. Molecular toxicity is caused by water-soluble compounds partitioning into the plasma membrane (PM) and interfering with membrane properties (9). Molecular toxicity is proportional to a solvent's aqueous concentration and reaches its maximum at a solvent's solubility point (i.e., at membrane and water saturation) (10). Phase toxicity occurs beyond a solvent's solubility and is defined as inhibition due to a distinct second phase (2). The molecular mechanisms of phase toxicity remain poorly understood, but we have demonstrated that limonene interferes with cell wall integrity (CWI) rather than membranes in *S. cerevisiae* (10). Accordingly, rational strategies for alleviating toxicity, such as manipulation of membrane fluidity or expression of membrane-bound solvent pumps, have failed to resolve the problem of phase toxicity (11).

In the past decade, adaptive laboratory evolution (ALE) (12, 13) has proven to be a successful technique for identifying biological solutions to combat alcohol (14, 15) and organic acid (16, 17) toxicity. Here we used ALE to identify genetic targets to alleviate phase toxicity. We describe a mutation in a single protein (tTcb3p$^{1-989}$) that can serve as a tool for the production of monoterpenes beyond their inhibitory limits.

MATERIALS AND METHODS

Strains, media, and chemicals. The *Saccharomyces cerevisiae* strain S288C (*MAT*α *SUC2 gal2 mal mel flo1 flo8-1 hap1*) was used as the parental strain and was provided by the Australian Wine Research Institute (AWRI), Adelaide, South Australia, Australia. A list of all strains used in this study can be found in Table S3 in the supplemental material. Δ*tcb3* and Δ*tcb2* knockout strains were derived from the BY4741 strain deletion collection (18). The genotype for the Δ*tcb3* strain is *MAT***a** *his3*Δ*1 leu2*Δ*0 met15*Δ*0 ura3*Δ*0 tcb3*Δ::*kanMX4*, and that for the Δ*tcb2* strain is *MAT***a** *his3*Δ*1 leu2*Δ*0 met15*Δ*0 ura3*Δ*0 tcb2*Δ::*kanMX4*. All chemicals were purchased from Sigma-Aldrich and were of analytical grade. The biojet fuel blend AMJ-700t was prepared in a 1-ml stock by mixing 50% (vol/vol) limonene, 10% (vol/vol) cymene, and 40% (vol/vol) farnesene. Unless otherwise noted, the synthetic medium (CBS) consisted of 2 g/liter sucrose, 5 g/liter $(NH_4)_2SO_4$, 3 g/liter KH_2PO_4, 0.5 g/liter $MgSO_4 \cdot 7H_2O$, and the vitamins and trace metals described in reference 2. Solid YPD medium consisted of 10 g/liter yeast extract, 10 g/liter polypeptone, and 20 g/liter sucrose. LM is YPD medium containing 300 mg/liter limonene. CBS$^+$

Received 18 December 2014 **Accepted** 26 February 2015

Accepted manuscript posted online 6 March 2015

Citation Brennan TCR, Williams TC, Schulz BL, Palfreyman RW, Krömer JO, Nielsen LK. 2015. Evolutionary engineering improves tolerance for replacement jet fuels in *Saccharomyces cerevisiae*. Appl Environ Microbiol 81:3316–3325. doi:10.1128/AEM.04144-14.

Editor: A. A. Brakhage

Address correspondence to Jens O. Krömer, j.kromer@uq.edu.au.

Supplemental material for this article may be found at http://dx.doi.org/10.1128/AEM.04144-14.

doi:10.1128/AEM.04144-14

medium is CBS medium modified by changing the concentration of sucrose to 5 g/liter and adding 20 mg/liter uracil, 50 mg/liter L-histidine, 50 mg/liter L-methionine, and 100 mg/liter L-leucine.

Adaptive evolution by serial batch passage. The parental strain (S288C) was transferred from a glycerol stock stored at −80°C and was grown on solid YPD medium at 30°C. A single colony of the parental strain was used to inoculate 10 ml of CBS medium, and this preculture was grown overnight until the mid-exponential-growth phase. The appropriate volume from the preculture was used to inoculate 22 ml of CBS medium in 250-ml Teflon-lined screw-top baffled shake flasks to a target optical density at 660 nm (OD_{660}) of 0.2. The initial volume of limonene added to the culture at inoculation was 1.0 μl (38 mg/liter). Limonene was directly added to the culture aseptically using a 10-μl glass syringe (Gerstel, Mülheim, Germany) immediately after inoculation. The culture was then incubated at 30°C and 200 rpm (in a Multitron orbital shaker with a 25-mm-diameter throw; Infors HT, Bottmingen, Switzerland) until it reached mid-exponential phase (OD_{660}, ~1 to 2, corresponding to ca. 3 doubling times). For the next round, the appropriate volume of the limonene-challenged culture was used to inoculate fresh medium (22 ml) to a target OD_{660} of 0.2. After several (2 to 4) transfers at a given limonene load, the amount of limonene was increased (between 0.2 and 0.5 μl [7.6 to 19 mg/liter] of additional limonene). After 52 daily sequential passages, the final limonene load was 5.8 μl (222 mg/liter). After each passage, 0.5 ml of culture (in the presence of limonene) was added to 0.5 ml of a 40% (vol/vol) glycerol solution, and the samples were stored at −80°C.

Screening of mutants. Mutants were screened by streaking frozen glycerol stocks out onto solid LM plates. The 8 to 12 largest single colonies were subjected to a second competitive growth screen in liquid CBS medium containing 95 mg/liter of limonene. Isolates were precultured in CBS medium (10 ml) overnight at 30°C (200 rpm), and the appropriate volume of the preculture was used to inoculate 22 ml of CBS to an OD_{660} of 0.2 in 250-ml Teflon-sealed screw-top shake flasks. Then 2.5 μl of limonene (95 mg/liter) was added immediately after inoculation, and growth was monitored for 12 h using a Libra S4 spectrophotometer at 660 nm. The mutant with the highest specific growth rate was chosen for tolerance testing.

Tolerance testing. The evolved and unevolved strains were evaluated for tolerance of each toxic compound as described in reference 2. Briefly, cultures were grown until mid-exponential phase (OD_{660}, ~1.0) and were then dosed with varying amounts of solvent. The optical density was evaluated for the ensuing 6 h. The MIC is defined as the amount of solvent required to inhibit the specific growth rate by approximately 50% relative to that of the control strain in the absence of solvents. For fitness tests, 3.6 μl (138 mg/liter) of limonene was added to the inoculum (22 ml at an OD_{660} of 0.2), and growth was monitored as described above. The ratio of the OD_{660} at 12 h to the OD_{660} at 0 h was used as a relative fitness metric for solvent tolerance (19). CBS medium containing 5 g/liter sucrose was used in all tolerance tests (CBS^+ medium was used for the Δ*tcb3* strain, and the fitness of the reconstructed tTcb3p, TB516, S288C, and BY4741 strains was also tested in CBS^+ medium [see Table S7 in the supplemental material]). All tolerance tests were performed in biological triplicate for each compound and strain.

DNA isolation. All DNA was isolated according to the method of Otero et al. (20) with the following modifications. A total of 5 ml of culture was harvested in mid-log phase (OD, ~3) at an RCF of 16,000 × *g* and 25°C, washed twice with distilled water, pelleted, and resuspended in 800 μl of lysis buffer (1% SDS, 50 mM EDTA, 0.1 M Tris-HCl [pH 7.5]). The suspension was transferred to FastPrep screw-cap tubes containing 1 g of 0.5-μm acid-washed beads and 100 μl of 5 M NaCl. To lyse the cells, four bead-beating cycles (30 s of beating followed by 1 min on ice) were carried out in a mechanical bead beater (John Morris Scientific, Pty Ltd., Sydney, Australia). The suspension was then harvested (RCF, 16,000 × *g*; 4°C) for 15 min, and the resulting clear liquid (ca. 800 μl) was transferred to new 1.5-ml UltraClean tubes (Mo Bio, Carlsbad, CA). Next, 777 μl of a chloroform–isoamyl alcohol (24:1) mixture was added and was incubated at 25°C for 30 min with gentle rocking. The mixture was then pelleted for 15 min (RCF, 16,000 × *g*; 25°C), and the top, aqueous layer was transferred to a new UltraClean tube, mixed with 70% (vol/vol) isopropanol, and centrifuged (RCF, 16,000 × *g*; 25°C) for 6 min. The isopropanol suspension was decanted, and the pellet was resuspended in 70% ethanol. The ethanol suspension was centrifuged (RCF, 16,000 × *g*; 25°C) for 6 min, and the pellet was allowed to dry for 45 min. The pellet was resuspended in 50 μl of DNA and RNA-free water containing 100 μg/ml RNase A and was incubated at room temperature for 30 min.

Genome sequencing. Paired-end (100-bp) genomic DNA libraries were generated using TruSeq DNA sample preparation kits according to the manufacturer's instructions (Illumina, San Diego, CA). Genomic DNA was sheared to a target insert size of 300 to 400 bp using a Covaris ultrasonicator (model M220; Covaris Inc., Woburn, MA). Whole-genome resequencing was performed by the Queensland Centre for Medical Genomics (Institute for Molecular Bioscience, University of Queensland, Brisbane, Australia) on an Illumina HiSeq 2500 system (HiSeq Control Software, version 2.0.5; RTA 1.17.20) by following the standard rapid sequencing workflow of cluster generation and sequencing by synthesis (SBS). Initially, libraries were loaded onto an Illumina cBot instrument for template hybridization and initial extension steps using the TruSeq Rapid Duo cBot sample loading kit (catalog no. CT-402-4001). Flow cells were then moved to the HiSeq 2500 instrument to complete cluster generation and sequencing using the TruSeq rapid paired-end cluster kit (catalog no. PE-402-4001) and the TruSeq rapid SBS kit (200 cycles) (catalog no. FC-402-4001) according to the manufacturer's publications. Samples were loaded at a concentration of 6 pM, and a total of 209 cycles of sequencing, consisting of two 101-bp reads and a single 7-bp index sequence, were completed.

For mutation analysis, the default settings in Bowtie 2 (version 2.0.2) and samtools (version 0.1.18) were used in alignment and mapping (21). The input paired-end reads (101 bp) were trimmed on the basis of quality (3 bases from the start and 23 bases from the end) to produce 75-bp reads for each sample. The results from the mapping were used to identify single nucleotide polymorphisms (SNPs) and insertions and deletions (indels) between the mutant and reference strain. The initial sequencing results and mutations, which were identified according to the default software settings mentioned above, are listed in Table S1 in the supplemental material. The mutations in Table S1 were further filtered, and alignments were viewed using Integrative Genomics Viewer (IGV) software (22). A mutation was called only if it met the following criteria: the mutation occurred in a coding region, and SNPs and indels were filtered using a Phred-like consensus quality of >30. For SNPs, the coverage depth was ≥10, and >95% of the base pair reads harbored the mutation. For indels, if the number of reads with an indel was less than the number of reads without it, that indel was filtered out. For example, initially, 39 mutations were identified in evolved strain TB302; however, after filtering, only 10 mutations occurred in coding regions, and 2 of them met the filtering criteria. Annotation and prediction of the effects caused by the mutations were carried out using the snpEff program (version 3.1) (23). The data were run against the Ensembl build (EF4.68) of the S288C reference genome and were used as input in the snpEff database.

Genomic reconstruction. The mutations in *PDR3* (Q763L) and *TCB3* (frameshift causing truncation at amino acid 989) were introduced into the parental strain (S288C) using the *amdSYM* recyclable dominant marker cassette (24). The reconstructed S288C strain harboring the mutation in *TCB3* resulting in truncation at amino acid 989 is referred to below as the tTcb3p strain. The details of construction can be found in the supplemental material (see Tables S2 and S8 in the supplemental material for primers and SNP reconstruction efficiency, respectively). A gain-of-function assay was performed for all reconstructed strains. As described above, relative fitness in the presence of limonene, cymene, β-pinene, myrcene, and AMJ-700t was investigated for the parental strain, an evolved strain (TB516), and reconstructed strains.

Fluorochrome staining and flow cytometry. For the S288C and tTcb3p strains, cell viability and cell wall damage were assessed using the vital staining dye propidium iodide (PI) and the cell wall binding dye calcofluor white (CFW). Briefly, cells were treated with an inhibitory amount of limonene (138 mg/liter) during the mid-log-growth phase (20 g/liter CBS medium). After 2 h of treatment, cell viability was tested (as described in reference 2), and cell wall staining was performed (as described in reference 10), in biological triplicate.

Transcriptomics. Total RNA was isolated from S288C and tTcb3p cultures during the mid-exponential-growth phase described previously (10). For control (no limonene) and limonene-challenged (107 mg/liter) cultures, approximately 10 ml of culture was quickly pelleted (RCF, 17,572 × *g*) for 2 min at 4°C, immediately resuspended in 2 ml of RNA*later* solution (Life Technologies, Carlsbad, CA), and stored at 4°C. The RiboPure-yeast kit (Ambion, Life Technologies, Carlsbad, CA) was used for total-RNA extraction according to the manufacturer's instructions, except that bead beating was used to lyse the cells, as described in reference 10. The RNA quality was assessed using an Agilent 2100 bioanalyzer and an RNA 6000 Nano kit according to the manufacturer's methods (Agilent, Santa Clara, CA). For the single-labeled microarrays (Affymetrix Yeast Genome 2.0 array), samples were labeled with 100 ng of total-RNA starting material by using the Affymetrix IVT Express labeling assay according to the manufacturer's instructions (Affymetrix, Santa Clara, CA). For hybridization, 4 μg of fragmented biotin-labeled cRNA was hybridized to each array at 45°C for 16 h at 60 rpm in an Affymetrix hybridization oven. Arrays were washed according to the manufacturer's instructions using an Affymetrix GeneChip Fluidics Station 450. Arrays were scanned using an Affymetrix S3000 scanner. The entire microarray processing procedure was performed at the Ramaciotti Centre for Gene Function Analysis (University of New South Wales, Sydney, Australia). Analysis of differentially expressed genes and gene set analysis (GSA) were carried out in R using the default values in the Piano package (25). All analysis was performed in biological triplicate.

Cell wall proteomics. The total cell wall extracts were isolated from S288C (parental strain) and tTcb3p cultures during the mid-exponential-growth phase. Cultures were inoculated to a starting OD_{660} of 0.1 in 22 ml of CBS medium (5 g/liter sucrose) and were allowed to grow to an OD_{660} of 1.0 in the absence or presence of limonene challenge (107 mg/liter). Approximately 20 ml of culture was pelleted (RCF, 4,025 × *g*; 5 min; room temperature), washed with sterile water, snap-frozen by quickly submerging the sample in dry ice for 2 min, and stored at −80°C. Cell wall protein was extracted by the method described in reference 26. Briefly, yeast cells were lysed with a bead beater; insoluble cell wall material was stringently washed; N-glycans were released with endo-β-*N*-acetylglucosaminidase H (endo H); and deglycosylated proteins covalently linked to the cell wall polysaccharide were digested with trypsin. Peptides were desalted with C_{18} ZipTips (Millipore) and were detected by liquid chromatography (LC)-electrospray ionization (ESI)-tandem mass spectrometry (MS-MS) with a Prominence nano LC system (Shimadzu) and a TripleTOF 5600 mass spectrometer with a Nanospray III interface (AB Sciex). For information-dependent acquisition (IDA), analyses were performed as described previously (27). Identical LC conditions were used for SWATH (sequential window acquisition of all theoretical mass spectra)-MS, with an MS–time of flight (TOF) scan from an *m/z* of 350 to an *m/z* of 1,800 for 0.05 s, followed by high-sensitivity information-independent acquisition with 26 *m/z* isolation windows, with 1 *m/z* window overlap, for 0.1 s across an *m/z* range of 400 to 1,250. The overall SWATH method is described in reference 28 and has been used successfully for proteomic quantification in yeast and other tissues without the use of wild-type–versus–wild-type statistical comparisons (29, 30). Collision energy was automatically assigned by Analyst software (AB Sciex) based on *m/z* window ranges. Proteins were identified from IDA data using ProteinPilot software (AB Sciex) as described previously (27). False-discovery-rate analysis using ProteinPilot was performed on all searches. Peptides identified with >99% confidence and with a local false-discovery rate of <1% were subjected to further analysis. *S. cerevisiae* cell wall proteins identified in these discovery data were used as the spectral library for analysis of SWATH MS-MS data using the SWATH processing script within PeakView, version 1.2 (AB SCIEX). The fragment ion peak area was used for quantification. The MSstats software package (31) was used for statistical analysis in R. The statistical significance cutoff was set at a P value of <0.05. All procedures were performed in biological triplicate.

Sequencing, transcriptome, and proteome data are available online (http://pathway.aibn.uq.edu.au/S288c/).

RESULTS

Evolved mutants show improved tolerance of limonene. Serial batch passaging was used to isolate limonene-tolerant yeast strains. The parental S288C strain underwent 52 daily sequential transfers under limonene stress. The limonene load increased from 38 mg/liter to 222 mg/liter. Tolerant strains were isolated as single colonies on plates during the adaptive evolution process and were tested for limonene tolerance. Two strains were isolated between generations 100 and 200, and four strains were isolated at 200 generations. Two tests were used to examine the improved fitness. The MIC (Table 1; see also Fig. S1 in the supplemental material) and relative fitness (Fig. 1) were measured for each strain and were compared to those of the parent. Relative fitness was defined as the ratio of the cell density (expressed as the OD_{660}) at 12 h to the cell density at 0 h under limonene exposure. All of the evolved strains showed at least a 1.8-fold increase in the MIC (Table 1) and at least a 9-fold increase in relative fitness in the presence of limonene (Fig. 1). The maximum relative fitness score (10.9 ± 1.6) was achieved at 120 generations (strain TB302) and did not increase significantly for later generations (generations 160 to 200 [Fig. 1]). In the absence of limonene, the maximum fitness score was 23.4 ± 0.4. For all strains and all tolerance tests, cell viability remained above 90% after 12 h of incubation (see Table S1 in the supplemental material). These results show that adaptive evolution employing serial batch transfer under constant limonene challenge was successful at isolating limonene-tolerant phenotypes.

Identification of mutations by whole-genome sequencing. Six resistant strains were isolated across the evolutionary time course in order to identify targets for genetic engineering. Mutations were identified by whole-genome resequencing, and each genome was compared with that of the parental strain, which was also sequenced and contained no mutations. For each evolved strain, we first identified all mutations occurring in coding regions. A summary of the sequencing results is presented in Table S1 in the supplemental material, and all of the mutations for each strain are listed in Table 1. The selection criteria for mutation calling are described in Materials and Methods. All resistant strains had a mutation (Q763L) in *PDR3*, while all strains with maximum fitness scores harbored an indel in either *TCB2* (deletion of amino acids 314 to 316 [strain TB302, isolated at 120 generations]) or the closely related gene *TCB3* (frameshift at bp 2966, resulting in the truncation of the protein to 989 amino acids) (Fig. 1). Considering that all of the other mutations found (Fig. 1 and Table 1) differed among the evolved strains, we assumed that these were passenger mutations arising from genetic drift and decided to focus our engineering efforts on the *PDR3* and *TCB3* mutations only. The genome data are available for download at http://pathway.aibn.uq.edu.au/S288c/.

Genomic reconstruction of the limonene-tolerant phenotype. We next constructed single and double mutations for the

TABLE 1 Summary of limonene MICs and mutations found in evolved strains

Strain	Gen[a]	MIC[b] (mg/liter)	FC[c]	Mutation	Gene	Function
S288C	0	69				
TB302	120	130	1.9	SNP (Q763L)	*PDR3*	Transcriptional activator of the pleiotropic drug resistance network
				Indel (deletions of E314, V315, P316)	*TCB2*	ER protein located in the mother and daughter bud, involved in ER-plasma membrane tethering
TB405	160	122	1.8	SNP (Q763L)	*PDR3*	Transcriptional activator of the pleiotropic drug resistance network
				Indel (frameshift; truncation at 989 aa)	*TCB3*	ER protein located in the mother and daughter bud, involved in ER-plasma membrane tethering
				Indel (frameshift; truncation at 192 aa)	*TSA1*	Thioredoxin peroxidase
				SNP (Q192G)		
				SNP (D380H)	*UBP11*	Ubiquitin-specific protease
TB511	200	138	2.0	SNP (Q763L)	*PDR3*	Transcriptional activator of the pleiotropic drug resistance network
				Indel (frameshift; truncation at 989 aa)	*TCB3*	ER protein located in the mother and daughter bud, involved in ER-plasma membrane tethering
				Indel (frameshift; truncation at 192 aa), SNP (Q192G)	*TSA1*	Thioredoxin peroxidase
				SNP (W580S)	*KSP1*	Serine/threonine protein kinase
				SNP (nonsense; Q1014*)	*PSE1*	Karyopherin/importin that interacts with the nuclear pore complex
				SNP (L84S)	*RPL30*	Ribosomal 60S subunit protein
TB516	200	138	2.0	SNP (Q763L)	*PDR3*	Transcriptional activator of the pleiotropic drug resistance network
				Indel (frameshift; truncation at 989 aa)	*TCB3*	ER protein located in the mother and daughter bud, involved in ER-plasma membrane tethering
				Indel, SNP (Q192G)	*TSA1*	Thioredoxin peroxidase
				SNP (R159T)	*CDC34*	Ubiquitin-conjugating enzyme; regulates cell cycle progression by targeting key substrates for degradation
TB517	200	145	2.1	SNP (Q763L)	*PDR3*	Transcriptional activator of the pleiotropic drug resistance network
				Indel (frameshift; truncation at 989 aa)	*TCB3*	ER protein located in the mother and daughter bud, involved in ER-plasma membrane tethering
				SNP (nonsense; Q1014*)	*PSE1*	Karyopherin/importin that interacts with the nuclear pore complex
				SNP (L84S)	*RPL30*	Ribosomal 60S subunit protein
TB519	200	138	2.0	SNP (Q763L)	*PDR3*	Transcriptional activator of the pleiotropic drug resistance network
				Indel (frameshift; truncation at 989 aa)	*TCB3*	ER protein located in the mother and daughter bud, involved in ER-plasma membrane tethering
				SNP (G826R)	*SIP3*	Transcription cofactor; acts through interaction with DNA-bound Snf1p
				SNP (L127F)	*YMR102c*	Protein of unknown function

[a] Gen, generation.
[b] Defined as the amount of limonene required to inhibit the specific growth rate by approximately 50% relative to the growth rate of the same strain in the absence of solvents.
[c] FC, fold change (ratio of the MIC for the evolved strain to the MIC for strain S288C).

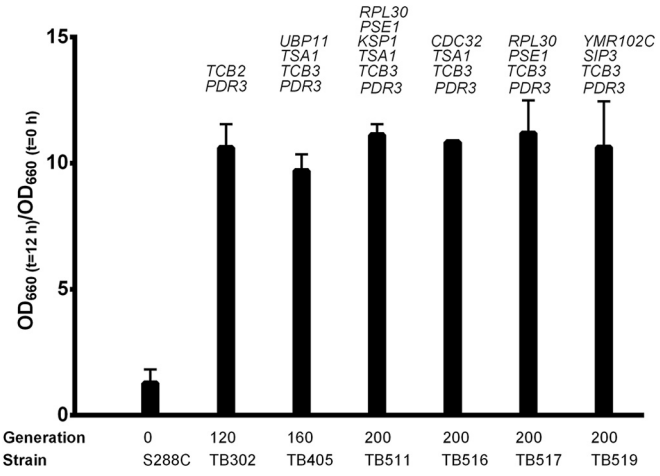

FIG 1 Summary of the relative fitness and genetic mutations of the evolved strains. Relative fitness is defined as the ratio of the cell density (expressed as the OD_{660}) at 12 h to the cell density at 0 h during limonene exposure (138 mg/liter). Error bars represent 1 SD above the mean for biological replicates ($n = 3$). The location of each mutation can be found in Table 1.

PDR3 (Q763L) and *TCB3* (frameshift resulting in truncation to 989 amino acids) genes in the parental strain and investigated the relative fitness of these mutants in a gain-of-function assay. A gain-of-function assay investigates whether a mutation confers a phenotype by reconstructing the mutation in the parent strain as opposed to evaluating the phenotype by knocking out genes systematically in an evolved strain. While the single base change $pdr3^{Q763L}$ conferred no significant improvement in fitness over the parental strain, the *tcb3-989* mutation (leading to truncated protein $tTcb3p^{1\text{-}989}$) increased limonene fitness 9-fold, and the strain with this mutation showed no statistical difference from the evolved strain (Fig. 2). The $pdr3^{Q763L}$ *tcb3-989* double mutant had a relative fitness score of 11.5 ± 0.5, which did not differ significantly from the fitness scores achieved by the evolved mutants or the *TCB3* single mutant (Fig. 2). The reconstructed double mutant carrying both the *TCB3* and *TCB2* mutations (*tcb3-989 tcb2-316*) showed no increase in fitness over that of the single $tTcb3p^{1\text{-}989}$ mutant (see Table S7 in the supplemental material). These data revealed that the mutation in $tTcb3p^{1\text{-}989}$ alone could confer limonene tolerance.

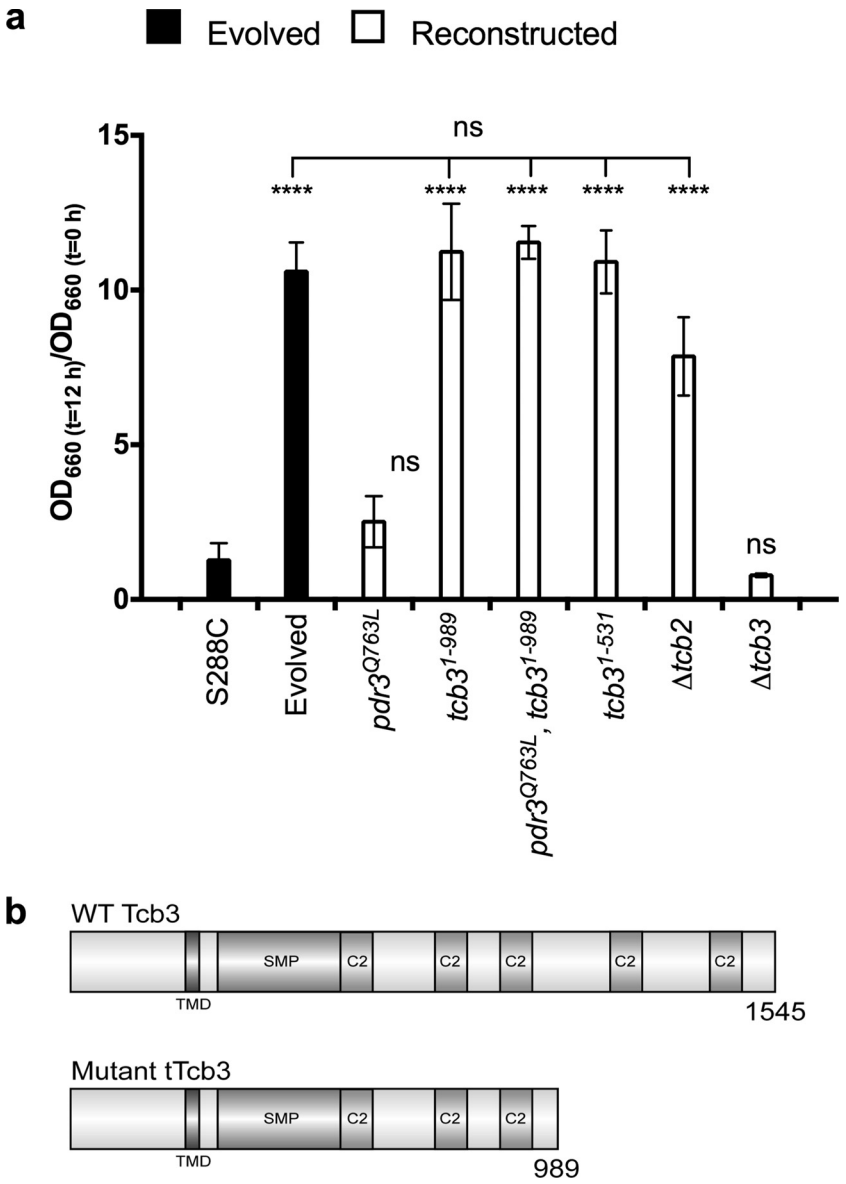

FIG 2 (a) Relative fitness of strains reconstructed with mutations in the presence of limonene. Relative fitness is defined in the legend to Fig. 1. The evolved strain score represents the average fitness score for all evolved strains (TB302 through TB519). Beneficial mutations in *PDR3* and *TCB3* were constructed in the parent strain (S288C). Error bars represent 1 SD from the mean for biological replicates ($n = 3$). Significance was determined by one-way analysis of variance to correct for multiple comparisons relative to the S288C result (****, $P < 0.001$; ns, not significant [$P > 0.05$]). (b) Diagram of S288C and the tTcb3p$^{1\text{-}989}$ mutant. The number of amino acids is given below each diagram. WT, wild type; TMD, transmembrane domain; SMP, synaptotagmin-like-mitochondrial lipid-binding protein; C2, lipid binding domain.

Given that the *TCB3* mutation encoded a truncated version of Tcb3p, we asked whether this mutation resulted in a nonfunctional protein and whether limonene resistance was due to effective loss of Tcb3p. A *TCB3* knockout strain, however, showed no enhanced tolerance and matched the fitness of S288C (Fig. 2a, Δ*tcb3*). This demonstrates that, despite encoding a truncated protein, the evolved tTcb3p strain has a gain-of-function mutation. This result further highlights the advantage of ALE over other approaches; traditional screening of knockout libraries would not have identified *TCB3* as a viable target.

Next, we investigated the potential biological implications of truncating Tcb3p. Normally, Tcb3p resides exclusively in the cortical endoplasmic reticulum (cER) and tethers the cER to the plasma membrane (PM) (32). It was recently demonstrated, however, that a truncated version of Tcb3p, lacking the C2 lipid binding domains (Fig. 2b, WT Tcb3), caused Tcb3p to untether itself from the PM and colocalize in the perinuclear endoplasmic reticulum (nER) and the cER. We investigated whether limonene resistance was associated with this dual localization property. We created a version of Tcb3p that was similarly truncated at position 531, which resulted in limonene tolerance (Fig. 2a, *tcb3*$^{1\text{-}531}$). These data strongly indicate that the gain of function and the resistant phenotype observed may be linked to the ability of tTcb3p to reside in both the cER and nER.

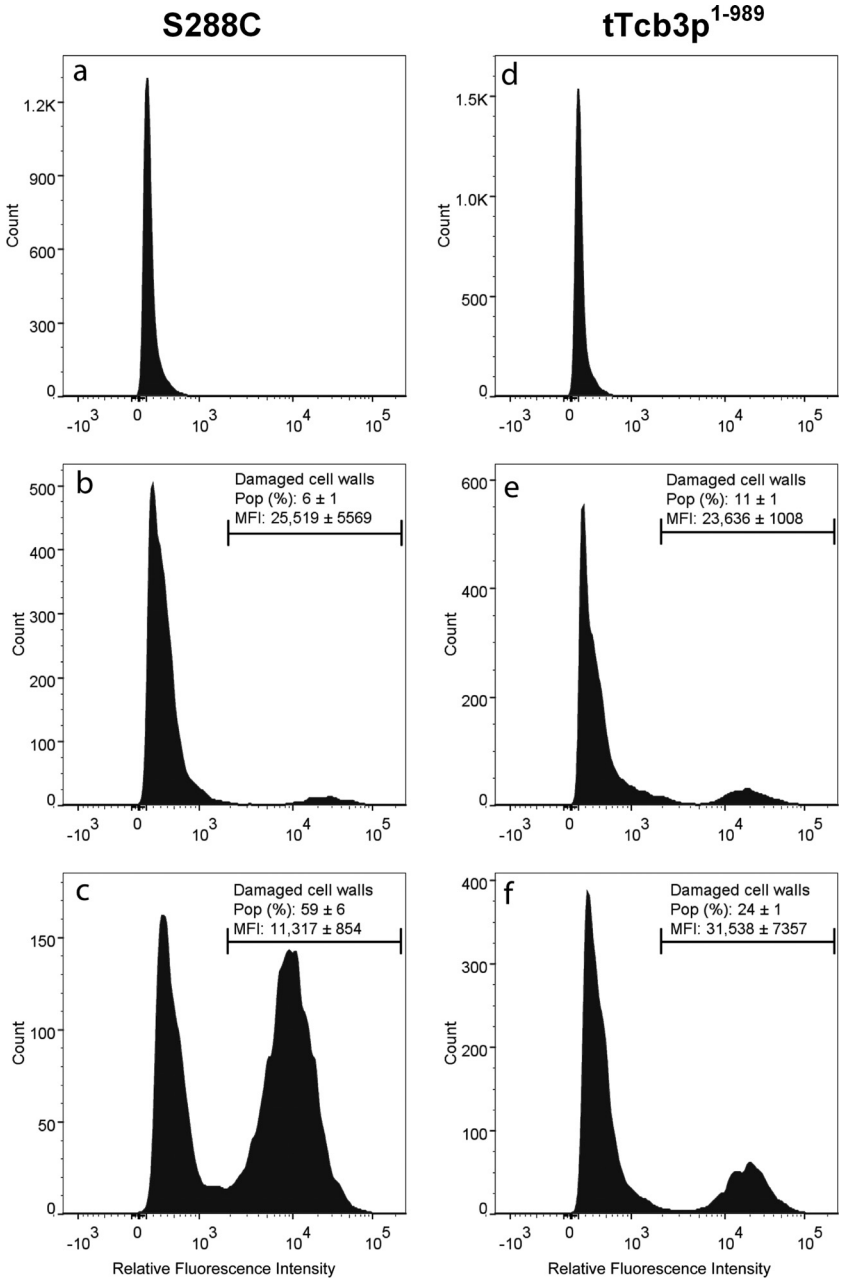

FIG 3 Histograms representing the variation in fluorescence emitted from S288C (wild-type) and tTcb3p$^{1\text{-}989}$ mutant cells. (a and d) Unstained cells; (b and e) unexposed control cells stained with CFW; (c and f) cells stained with CFW after 2 h of limonene exposure. The mean fluorescence intensity (MFI) and mean percentage of damaged cells (Pop %) ± SD are reported for biological replicates ($n = 3$).

Alternatively, limonene resistance may also be due to the loss of the tricalbin complex. Tcb2p forms a heterocomplex with Tcb3p (and Tcb1p) by binding to the C-terminal portions of tricalbins 1 and 3 (33). With the C terminus of Tcb3p absent in both truncated versions (ending at position 989 or 531), we questioned if limonene resistance was associated with the breakdown of the Tcb2p-Tcb3p tricalbin complex. A full knockout of Tcb2p was effective at increasing limonene resistance (Fig. 2a, Δ*tcb2* [fitness score, 7.86 ± 1.27]). In addition to the dual localization property of Tcb3p in the ER, the absence of the tricalbin complex may also contribute to the resistance mechanism.

Changes to CWI, the transcriptome, and the proteome. We demonstrated previously that limonene damages the cell wall (10). Hence, we explored if the tTcb3p$^{1\text{-}989}$ mutation improved the structural integrity of the cell wall during limonene stress. Cell wall integrity (CWI) was measured using calcofluor white (CFW), a fluorochrome that binds to cell wall polysaccharides (34). Cells with damaged walls show increased sensitivity and a higher mean fluorescence intensity (MFI) when stained with CFW (10). As shown in Fig. 3c, 59% ± 6% of S288C cells had substantial cell wall damage after limonene exposure. This was a 10-fold increase in the proportion of damaged cells over that for the untreated control

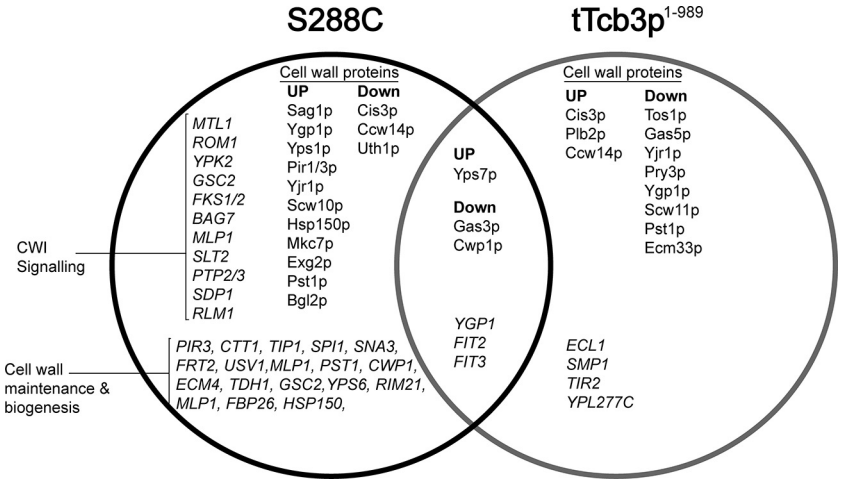

FIG 4 Cell wall transcriptome and proteome responses during limonene stress. Venn diagrams represent overlaps and differences in cell wall gene expression (upregulated genes only) and protein abundance between S288C and tTcb3p$^{1-989}$ cells. Cell wall genes upregulated in S288C are from the work of Brennan et al. (10). Genes upregulated in the tTcb3p$^{1-989}$ mutant, and cell wall proteins with changes in expression in S288C or the tTcb3p$^{1-989}$ mutant, were analyzed in this study.

(6% ± 1% [Fig. 3b]). In contrast, cells harboring the tTcb3p$^{1-989}$ single mutation showed a much smaller, 2-fold increase in cell wall damage after limonene treatment (24% ± 1% versus 11% ± 1% of cells damaged [Fig. 3e and f]). In addition, loss of cell wall integrity affected cytokinesis, and the number of defects in cell separation was found to be higher in treated S288C cells than in treated tTcb3p$^{1-989}$ cells (see Fig. S3 in the supplemental material). These results demonstrate that the tTcb3p$^{1-989}$ protein has the ability to preserve cell wall integrity during limonene treatment.

In wild-type strains, limonene exposure causes a substantial transcriptional response (10). When strains were challenged with limonene, the total number of differentially expressed genes (29 genes) (see Table S4 in the supplemental material) was substantially lower for the tTcb3p$^{1-989}$ strain than for strain S288C (453 genes reported in reference 10). This is partly explained by the large number of regulated genes associated with growth defects in S288C (10). The tTcb3p$^{1-989}$ mutant showed very small perturbations to growth when challenged with limonene, and thus, the smaller gene list was not surprising (see Fig. S2 in the supplemental material). However, roughly 30% of genes on the upregulated-gene list are associated with cell wall repair (see Table S4). In yeast, the CWI signaling pathway is responsible for responding to cell wall damage (35). The CWI cascade was highly upregulated in S288C (10) but was not induced in mutant cells (Fig. 4). In tTcb3p$^{1-989}$ cells, limonene stress induced genes associated with cell wall maintenance, which are not part of the CWI signaling pathway. *ECL1*, *SMP1*, *TIR2*, and *YPL277C* were upregulated in the mutant but not in S288C, and only three upregulated genes were shared by the strains (*YGP1*, *FIT2*, *FIT3*). Several genes involved in iron ion homeostasis were also upregulated (*SIT1*, *HMX1*, *ARN1*, *FRE5*, *TIS11*). This response was similarly observed for exposed S288C cells (10). Global transcript analysis was also performed in the absence of limonene to investigate expression patterns directly caused by the *TCB3* mutation (comparing gene expression by the tTcb3p$^{1-989}$ mutant with that by S288C). However, no genes were differentially expressed.

We also characterized the direct impact of the tTcb3p$^{1-989}$ mutation on cell wall protein abundance during limonene shock. For untreated cells, Ygp1p was the only protein induced in the mutant relative to S288C (see Table S5 in the supplemental material). The cell wall proteins Plb1p, Plb2p, Ecm33p, Tos1p, Cis3p, and Uth1p were found to be lower in abundance in the mutant than in S288C (see Table S5). During limonene challenge, the cell wall proteins Pbl2p, Cis3p, and Ccw14p were induced in the mutant but were absent in the parental strain. Gas3p, Yap7p, and Cwp1p were the only common regulated cell wall proteins found during limonene stress (Fig. 4). Taken together, these data demonstrate that both the *TCB3* mutation and limonene affect protein secretion or cell wall biosynthesis, but in different ways. The underlying mechanisms, however, remain unresolved.

Tolerance toward terpenes other than limonene. To test if the tTcb3p$^{1-989}$ mutation also conferred tolerance toward terpenes other than limonene, the tolerance assays were repeated with a range of compounds. Fitness in the presence of β-pinene and myrcene increased significantly (11- and 8-fold, respectively) over that of S288C (Fig. 5), and the fitness of the reconstructed strain matched, or was improved over, that of the evolved strain (TB516). The mutant showed no fitness increase in the presence of the aromatic monoterpene cymene (Fig. 5) or of other aromatics (xylene, toluene, and styrene [see Table S6 in the supplemental material]). A 4-fold increase was observed in tolerance of a terpene jet fuel precursor mixture (AMJ-700t) (Fig. 5). AMJ-700t contains, by volume, 50% limonene, 10% cymene, and 40% farnesene. After a single hydrogenation step, AMJ-700t can be converted to the paraffin jet fuel mixture AMJ-700 (50% limonane, 10% cymene, and 40% farnesane), which was successfully used in a demonstration flight during Rio+20 in June 2012 (42).

DISCUSSION

Strains with improved fitness in the presence of limonene and other toxic terpenes were identified through adaptive evolution employing serial batch passaging (Fig. 1 and 5). In typical ALE approaches, the final strain is sequenced and is compared with the parent strain (19). Here we resequenced genomes across the evolutionary time course and constructed a spatiotemporal representation of the environmentally selected mutations. This enabled us

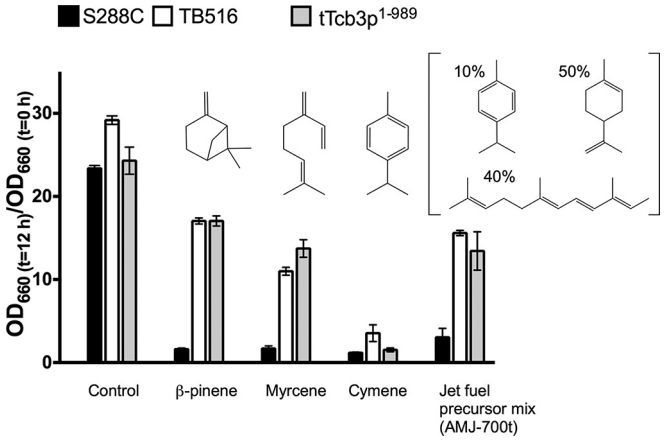

FIG 5 Relative fitness in the presence of terpenes other than limonene. S288C, an evolved strain (TB516), and the reconstructed tTcb3p$^{1-989}$ strain were subjected to relative fitness assays for β-pinene (198 mg/liter), myrcene (361 mg/liter), cymene (140 mg/liter), and AMJ-700t (225 mg/liter). AMJ-700t contains, by volume, 10% cymene, 50% limonene, and 40% farnesene. Control bars represent no exposure. Relative fitness is defined in the legend to Fig. 1. Error bars represent 1 SD from the mean for biological replicates ($n = 3$).

to judge more precisely which mutations were potentially significant. For example, if TB511 had been the only final strain sequenced, then six potential gene targets would have had to been examined. Alternatively, we captured mutations in *TCB2/TCB3* and *PDR3* that occurred early on in ALE (Fig. 1). When the final evolved strains (TB511 to TB519) were analyzed, this information was useful for deciding which genes to focus on for strain development.

For example, a mutation in *PDR3*, encoding the transcriptional activator for the pleiotropic drug resistance network, was found in every evolved strain (Fig. 1). Upregulation of ABC transporters during limonene stress has been observed previously, but overexpression of these failed to improve limonene tolerance (11). Similarly, we observed that a genomic reconstruction of the mutation (*pdr3*^{Q763L}) in S288C did not significantly improve fitness (Fig. 2a). The transporters may address low levels of molecular toxicity while failing to address the major issue of phase toxicity.

Mutations in the tricalbin ("tri" for three, "ca" for calcium, "l" for lipid, and "bin" for binding) (33) protein Tcb2p or Tcb3p were found in all evolved strains with maximum fitness scores (Fig. 1). A mutation in *TCB2* was found early (at 120 generations; strain TB302 in Fig. 1), while an indel in *TCB3* causing truncation at position 989 was found at later time points. Genomic reconstruction of *tcb3-989* in S288C revealed that the limonene-resistant phenotype can be achieved by this single point mutation. The correlation of genotype with phenotype is generally a complex problem (36). To our knowledge, no previous report has described a single point mutation that confers tolerance toward toxic next-generation biofuels on yeast.

While the specific role of the *TCB3* mutation remains unresolved, this work shows that it is involved in preventing cell wall damage. Limonene stress causes reduced cell wall integrity in S288C (Fig. 3c) and strongly induces the cell wall integrity signaling pathway (Fig. 4). In the reconstructed strain, limonene did not severely affect cell wall integrity (Fig. 3f), and there was no activation of CWI signaling during limonene shock (Fig. 4). Limonene had different and, in several instances, opposite effects on the cell wall proteome, while fewer genes involved in cell wall maintenance and biogenesis were affected in the tTcb3p$^{1-989}$ variant (Fig. 4). The mutation may directly enhance cell wall resilience, e.g., by increasing the degree of cross-linking. For example, Cis3p and Ccw14p serve as structural stabilizers covalently linking cell wall polysaccharides (37, 38) and were upregulated in the mutant but not in S288C (Fig. 4). Enhanced cell wall protection in the mutant was evident after investigation of budding patterns during limonene stress (see Fig. S3 in the supplemental material).

In addition to biofuel applications, this work has revealed new insights into the biological function of tricalbin proteins, which are homologous to synaptotagmins and SNARE proteins in mammalian cells (39). Little is known about the biological function of tricalbins other than that they can tether the ER to the plasma membrane (32, 39). This study links tricalbins to the regulation of cell wall integrity, which has not been reported previously. The data also show that when tricalbins act as heterodimers rather than as free proteins, different biological behavior is observed *in vivo*. This work serves as a foundation for future studies to explore the mechanism and functional implications of this distinction between complexed and noncomplexed tricalbins.

Commercial-level biological production of monoterpenes depends on solving the toxicity problem. Currently, monoterpene olefin production in yeast is still in the developmental stage, and titers have yet to reach inhibitory levels (60 to 200 mg/liter). As strain engineering leads to better-performing strains, phase toxicity will become a major constraint. Monoterpenes passively diffuse in and out of cells (40, 41), which means that high endogenous cellular production will drive transport to the extracellular environment, increasing the solvent phase and enhancing phase toxicity effects. This is the first example of successful engineering of phase tolerance and the first report of a single point mutation that confers tolerance of a range of toxic next-generation biofuels. Given the simplicity of the Tcb3p mutation, our work provides a straightforward strategy that can be tailored to any yeast strain to increase tolerance, with direct applications to biocatalysis or biotransformation of toxic alkenes.

ACKNOWLEDGMENTS

We thank the Queensland government (National and International Research Alliances Program) for financial support. J.O.K. was financially supported by the Australian Research Council (DE120101549). B.L.S. was financially supported by a National Health and Medical Research Council Career Development Fellowship (APP1031542).

We thank the Australian Wine Research Institute (Adelaide, South Australia, Australia) for providing us with the S288C yeast strain. We thank Chris Paddon (Amyris Inc., Emeryville, CA), Amir Feizi, and Jens Nielsen (Chalmers University of Technology, Gothenburg, Sweden) for useful discussions, Amelia Tuffley (University of Queensland) for technical assistance with cell wall extraction, and Tim Mercer (Garvan Institute, UNSW, Australia) for reviewing the manuscript. Whole-genome resequencing was performed by the Queensland Centre for Medical Genomics (Institute for Molecular Bioscience, University of Queensland, St. Lucia, Queensland, Australia). Transcriptomics was performed at the Ramaciotti Centre for Gene Function Analysis (University of New South Wales, Sydney, Australia). Microscopy was performed at the Australian National Fabrication Facility (ANFF) (University of Queensland, St. Lucia, Queensland, Australia).

We declare no competing financial interests.

REFERENCES

1. **Keasling J.** 2008. Synthetic biology for synthetic chemistry. ACS Chem Biol **3:**64–76. http://dx.doi.org/10.1021/cb7002434.
2. **Brennan TCR, Turner CD, Krömer JO, Nielsen LK.** 2012. Alleviating monoterpene toxicity using a two-phase extractive fermentation for the bioproduction of jet fuel mixtures in *Saccharomyces cerevisiae*. Biotechnol Bioeng **109:**2513–2522. http://dx.doi.org/10.1002/bit.24536.
3. **Fischer MJC, Meyer S, Claudel P, Bergdoll M, Karst F.** 2011. Metabolic engineering of monoterpene synthesis in yeast. Biotechnol Bioeng **108:** 1883–1892. http://dx.doi.org/10.1002/bit.23129.
4. **Lücker J, El Tamer MK, Schwab W, Verstappen FWA, van der Plas LHW, Bouwmeester HJ, Verhoeven HA.** 2002. Monoterpene biosynthesis in lemon (*Citrus limon*). cDNA isolation and functional analysis of four monoterpene synthases. Eur J Biochem **269:**3160–3171. http://dx.doi.org/10.1046/j.1432-1033.2002.02985.x.
5. **Rico J, Pardo E, Orejas M.** 2010. Enhanced production of a plant monoterpene by overexpression of the 3-hydroxy-3-methylglutaryl coenzyme A reductase catalytic domain in *Saccharomyces cerevisiae*. Appl Environ Microbiol **76:**6449–6454. http://dx.doi.org/10.1128/AEM.02987-09.
6. **Chang M, Keasling J.** 2006. Production of isoprenoid pharmaceuticals by engineered microbes. Nat Chem Biol **2:**674–681. http://dx.doi.org/10.1038/nchembio836.
7. **Hill J, Nelson E, Tilman D, Polasky S, Tiffany D.** 2006. Environmental, economic, and energetic costs and benefits of biodiesel and ethanol biofuels. Proc Natl Acad Sci U S A **103:**11206–11210. http://dx.doi.org/10.1073/pnas.0604600103.
8. **Khor GK, Uzir MH.** 2011. *Saccharomyces cerevisiae*: a potential stereospecific reduction tool for biotransformation of mono- and sesquiterpenoids. Yeast **28:**93–107. http://dx.doi.org/10.1002/yea.1827.
9. **Sikkema J, de Bont JA, Poolman B.** 1994. Interactions of cyclic hydrocarbons with biological membranes. J Biol Chem **269:**8022–8028.
10. **Brennan TCR, Krömer JO, Nielsen LK.** 2013. Physiological and transcriptional responses of *Saccharomyces cerevisiae* to *d*-limonene show changes to the cell wall but not to the plasma membrane. Appl Environ Microbiol **79:**3590–3600. http://dx.doi.org/10.1128/AEM.00463-13.
11. **Hu F, Liu J, Du G, Hua Z, Zhou J, Chen J.** 2012. Key cytomembrane ABC transporters of *Saccharomyces cerevisiae* fail to improve the tolerance to *d*-limonene. Biotechnol Lett **34:**1505–1509. http://dx.doi.org/10.1007/s10529-012-0931-6.
12. **Çakar ZP, Turanlı-Yıldız B, Alkım C, Yılmaz Ü.** 2012. Evolutionary engineering of *Saccharomyces cerevisiae* for improved industrially important properties. FEMS Yeast Res **12:**171–182. http://dx.doi.org/10.1111/j.1567-1364.2011.00775.x.
13. **Portnoy VA, Bezdan D, Zengler K.** 2011. Adaptive laboratory evolution—harnessing the power of biology for metabolic engineering. Curr Opin Biotechnol **22:**590–594. http://dx.doi.org/10.1016/j.copbio.2011.03.007.
14. **Atsumi S, Hanai T, Liao JC.** 2008. Non-fermentative pathways for synthesis of branched-chain higher alcohols as biofuels. Nature **451:**86–89. http://dx.doi.org/10.1038/nature06450.
15. **Brown SD, Guss AM, Karpinets TV, Parks JM, Smolin N, Yang S, Land ML, Klingeman DM, Bhandiwad A, Rodriguez M, Raman B, Shao X, Mielenz JR, Smith JC, Keller M, Lynd LR.** 2011. Mutant alcohol dehydrogenase leads to improved ethanol tolerance in *Clostridium thermocellum*. Proc Natl Acad Sci U S A **108:**13752–13757. http://dx.doi.org/10.1073/pnas.1102444108.
16. **Jantama K, Haupt MJ, Svoronos SA, Zhang X, Moore JC, Shanmugam KT, Ingram LO.** 2008. Combining metabolic engineering and metabolic evolution to develop nonrecombinant strains of *Escherichia coli* C that produce succinate and malate. Biotechnol Bioeng **99:**1140–1153. http://dx.doi.org/10.1002/bit.21694.
17. **Wright J, Bellissimi E, de Hulster E, Wagner A, Pronk JT, van Maris AJA.** 2011. Batch and continuous culture-based selection strategies for acetic acid tolerance in xylose-fermenting *Saccharomyces cerevisiae*. FEMS Yeast Res **11:**299–306. http://dx.doi.org/10.1111/j.1567-1364.2011.00719.x.
18. **Giaever G, Chu AM, Ni L, Connelly C, Riles L, Veronneau S, Dow S, Lucau-Danila A, Anderson K, Andre B, Arkin AP, Astromoff A, El-Bakkoury M, Bangham R, Benito R, Brachat S, Campanaro S, Curtiss M, Davis K, Deutschbauer A, Entian KD, Flaherty P, Foury F, Garfinkel DJ, Gerstein M, Gotte D, Guldener U, Hegemann JH, Hempel S, Herman Z, Jaramillo DF, Kelly DE, Kelly SL, Kotter P, LaBonte D, Lamb DC, Lan N, Liang H, Liao H, Liu L, Luo C, Lussier M, Mao R, Menard P, Ooi SL, Revuelta JL, Roberts CJ, Rose M, Ross-Macdonald P, Scherens B, et al.** 2002. Functional profiling of the *Saccharomyces cerevisiae* genome. Nature **418:**387–391. http://dx.doi.org/10.1038/nature00935.
19. **Atsumi S, Wu T-Y, Machado IMP, Huang W-C, Chen P-Y, Pellegrini M, Liao JC.** 2010. Evolution, genomic analysis, and reconstruction of isobutanol tolerance in *Escherichia coli*. Mol Syst Biol **6:**449. http://dx.doi.org/10.1038/msb.2010.98.
20. **Otero J, Vongsangnak W, Asadollahi M, Olivares-Hernandes R, Maury J, Farinelli L, Barlocher L, Osteras M, Schalk M, Clark A, Nielsen J.** 2010. Whole genome sequencing of *Saccharomyces cerevisiae*: from genotype to phenotype for improved metabolic engineering applications. BMC Genomics **11:**723. http://dx.doi.org/10.1186/1471-2164-11-723.
21. **Langmead B, Salzberg SL.** 2012. Fast gapped-read alignment with Bowtie 2. Nat Methods **9:**357–359. http://dx.doi.org/10.1038/nmeth.1923.
22. **Robinson JT, Thorvaldsdottir H, Winckler W, Guttman M, Lander ES, Getz G, Mesirov JP.** 2011. Integrative genomics viewer. Nat Biotechnol **29:**24–26. http://dx.doi.org/10.1038/nbt.1754.
23. **Cingolani P, Platts A, Wang LL, Coon M, Tung N, Wang L, Land SJ, Lu X, Ruden DM.** 2012. A program for annotating and predicting the effects of single nucleotide polymorphisms, SnpEff: SNPs in the genome of *Drosophila melanogaster* strain w^{1118}; *iso-2*; *iso-3*. Fly **6:**80–92. http://dx.doi.org/10.4161/fly.19695.
24. **Solis-Escalante D, Kuijpers NGA, Bongaerts N, Bolat I, Bosman L, Pronk JT, Daran J-M, Daran-Lapujade P.** 2013. amdSYM, a new dominant recyclable marker cassette for *Saccharomyces cerevisiae*. FEMS Yeast Res **13:**126–139. http://dx.doi.org/10.1111/1567-1364.12024.
25. **Väremo L, Nielsen J, Nookaew I.** 2013. Enriching the gene set analysis of genome-wide data by incorporating directionality of gene expression and combining statistical hypotheses and methods. Nucleic Acids Res **41:** 4378–4391. http://dx.doi.org/10.1093/nar/gkt111.
26. **Schulz BL, Aebi M.** 2009. Analysis of glycosylation site occupancy reveals a role for Ost3p and Ost6p in site-specific *N*-glycosylation efficiency. Mol Cell Proteomics **8:**357–364. http://dx.doi.org/10.1074/mcp.M800219-MCP200.
27. **Bailey UM, Jamaluddin MF, Schulz BL.** 2012. Analysis of congenital disorder of glycosylation-Id in a yeast model system shows diverse site-specific under-glycosylation of glycoproteins. J Proteome Res **11:**5376–5383. http://dx.doi.org/10.1021/pr300599f.
28. **Gillet LC, Navarro P, Tate S, Rost H, Selevsek N, Reiter L, Bonner R, Aebersold R.** 2012. Targeted data extraction of the MS/MS spectra generated by data-independent acquisition: a new concept for consistent and accurate proteome analysis. Mol Cell Proteomics **11:**O111.016717. http://dx.doi.org/10.1074/mcp.O111.016717.
29. **Liu Y, Chen J, Sethi A, Li QK, Chen L, Collins B, Gillet LC, Wollscheid B, Zhang H, Aebersold R.** 2014. Glycoproteomic analysis of prostate cancer tissues by SWATH mass spectrometry discovers *N*-acylethanolamine acid amidase and protein tyrosine kinase 7 as signatures for tumor aggressiveness. Mol Cell Proteomics **13:**1753–1768. http://dx.doi.org/10.1074/mcp.M114.038273.
30. **Sullivan M, Li S, Aroney S, Deng B, Li C, Roura E, Schulz B, Harcourt B, Forbes J, Gilbert R.** 2015. A rapid extraction method for glycogen from formalin-fixed liver. Carbohydr Polym **118:**9–15. http://dx.doi.org/10.1016/j.carbpol.2014.11.005.
31. **Choi M, Chang C-Y, Vitek O.** 20 September 2013. Package 'MSstats.' Protein significance analysis in LC-MS, SRM and DIA for label-free or label-based proteomics experiments, version 2.0.1. http://www.bioconductor.org/packages/2.13/bioc/manuals/MSstats/man/MSstats.pdf.
32. **Manford AG, Stefan CJ, Yuan HL, MacGurn JA, Emr SD.** 2012. ER-to-plasma membrane tethering proteins regulate cell signaling and ER morphology. Dev Cell **23:**1129–1140. http://dx.doi.org/10.1016/j.devcel.2012.11.004.
33. **Creutz CE, Snyder SL, Schulz TA.** 2004. Characterization of the yeast tricalbins: membrane-bound multi-C2-domain proteins that form complexes involved in membrane trafficking. Cell Mol Life Sci **61:**1208–1220. http://dx.doi.org/10.1007/s00018-004-4029-8.
34. **Ram AF, Klis FM.** 2006. Identification of fungal cell wall mutants using susceptibility assays based on Calcofluor white and Congo red. Nat Protoc **1:**2253–2256. http://dx.doi.org/10.1038/nprot.2006.397.

35. **Levin DE.** 2011. Regulation of cell wall biogenesis in *Saccharomyces cerevisiae*: the cell wall integrity signaling pathway. Genetics **189:**1145–1175. http://dx.doi.org/10.1534/genetics.111.128264.
36. **Dowell RD, Ryan O, Jansen A, Cheung D, Agarwala S, Danford T, Bernstein DA, Rolfe PA, Heisler LE, Chin B, Nislow C, Giaever G, Phillips PC, Fink GR, Gifford DK, Boone C.** 2010. Genotype to phenotype: a complex problem. Science **328:**469. http://dx.doi.org/10.1126/science.1189015.
37. **Moukadiri I, Armero J, Abad A, Sentandreu R, Zueco J.** 1997. Identification of a mannoprotein present in the inner layer of the cell wall of *Saccharomyces cerevisiae*. J Bacteriol **179:**2154–2162.
38. **Mrsa V, Ecker M, Strahl-Bolsinger S, Nimtz M, Lehle L, Tanner W.** 1999. Deletion of new covalently linked cell wall glycoproteins alters the electrophoretic mobility of phosphorylated wall components of *Saccharomyces cerevisiae*. J Bacteriol **181:**3076–3086.
39. **Toulmay A, Prinz WA.** 2012. A conserved membrane-binding domain targets proteins to organelle contact sites. J Cell Sci **125:**49–58. http://dx.doi.org/10.1242/jcs.085118.
40. **Bishop JR, Nelson G, Lamb J.** 1998. Microencapsulation in yeast cells. J Microencapsul **15:**761–773. http://dx.doi.org/10.3109/02652049809008259.
41. **Ciamponi F, Duckham C, Tirelli N.** 2012. Yeast cells as microcapsules. Analytical tools and process variables in the encapsulation of hydrophobes in *S. cerevisiae*. Appl Microbiol Biotechnol **95:**1445–1456. http://dx.doi.org/10.1007/s00253-012-4127-8.
42. **Amyris.** 19 June 2012. Photo release—Azul Brazilian Airlines makes successful demonstration flight with Amyris renewable jet fuel produced from sugarcane. [Press release.] Retrieved from https://amyris.com/photo-release-azul-brazilian-airlines-makes-successful-demonstration-flight-with-amyris-renewable-jet-fuel-produced-from-sugarcane/.